

The electrometer concept and binding of cations to phospholipid bilayers

Andrea Catte,^{*} Mykhailo Girykh,[†] Matti Javanainen,[‡] Markus S. Miettinen,[§] Luca Monticelli,[¶]
Jukka Määttä,^{**} Vasily S. Oganessian,^{††} O. H. Samuli Ollila,^{‡‡} and Joona Tynkkynen[‡]

Despite of vast amount of experimental and theoretical studies, the binding affinity of cations, especially the biologically relevant Na^+ and Ca^{2+} ions, into a phospholipid bilayer is not agreed on in the literature. Here we show that the ion binding affinity can be directly compared between simulations and experiments by using the choline headgroup order parameters according to the electrometer concept. Our results strongly support the traditional view that Na^+ ions and other monovalent ions (except Li^+) do not specifically bind to phosphatidylcholine lipid bilayers with mM concentrations, in contrast to Ca^{2+} and other multivalent ions. Especially the Na^+ binding affinity is overestimated by several molecular dynamics simulation models, leading to artificially positively charged lipid bilayer. Qualitatively correct headgroup order parameter response is observed with Ca^{2+} binding in all the tested models, however none of the tested models has sufficient quantitative accuracy to interpret the Ca^{2+} /lipid stoichiometry or induced atomistic resolution structural changes.

This work has been, and continues to be, progressed and discussed through the blog: nmrlipids.blogspot.fi. Everyone is invited to join the discussion and make contributions through the blog. The manuscript will be eventually submitted to an appropriate scientific journal. Everyone who has contributed to the work through the blog will be offered coauthorship. For more details see: nmrlipids.blogspot.fi.

I. INTRODUCTION

The cation interactions with phospholipid membranes occur in a large amount of physiological processes, nerve cell signalling being the prime example. Thus, the interactions between different cations and phospholipid bilayers have been widely studied by experiments and theory. While it is practically agreed that the relative binding affinity of different ions follows the Hofmeister series [1–9], the quantitative binding affinities of different ions are not agreed on in the literature. The extensive reviews of the work done prior 1990 [2, 3] concluded that monovalent cations (Li^+ being an exception) interact only weakly with phospholipid bilayers, while for multivalent ions the interactions are significant. This conclusion has been supported by further studies where the bilayer properties have remained intact mM concentrations of monovalent salt [4, 10, 11]. On the other hand, the weak interactions with monovalent ions have been questioned in several experimental and molecular dynamics simulation studies [6–9, 12–18] suggesting stronger binding especially for Na^+ ions.

More specifically, mM concentrations NaCl has a negligible effect on the choline headgroup order parameters [19], area per molecule [10], dipole potential [20], and lipid lateral diffusion [11]; in contrast, these properties are significantly affected by the presense of CaCl_2 or other multivalent ions. In addition, water sorption isotherm for POPC/NaCl system was essentially similar to NaCl in pure water—indicating only weak interaction between ion and lipid [4]. Only minor changes in POPC infrared spectra were observed in the presense of NaCl compared to the significant changes in the presense of Ca^{2+} and other multivalent ions, and it was again concluded that the Na^+ -lipid interactions are weak [4].

In contrast, decrease of fluorescent probe rotational and translational dynamics in lipid bilayer with mM NaCl concentrations suggested significant Na^+ binding [7, 9, 12]. However, the reduced lateral diffusion is not observed in non-invasive NMR experiments, suggesting that fluorescence results arise from Na^+ interactions with probes rather than with lipids [11]. Also the interpretation of calorimetric measurements has been controversial: Previously the small effect of monovalent ions (except Li^+) on phase transition temperature compared to multivalent ions was interpreted such that only multivalent ions and Li^+ specifically bind to phospholipid bilayer [2], however, more recently the small changes in calorimetric experiments have been interpreted to indicate also Na^+ binding [8, 12]. In electrophoresis measurements of phosphatidylcholine vesicles, NaCl can increase the originally negative zeta potential close to zero, however, positive zeta potential can be typically reached only with multivalent ions or Li^+ [1, 8, 14, 15, 21]. The lack of significant positive electrophoretic mobility in the presence of NaCl has been recognized to contradict with suggested strong binding of Na^+ , however the contradiction has been explained by the effect of Cl^- ions to the electrophoretic mobility [22, 23]. Also changes in bilayer hardness and area per lipid measured with Atomistic Force Microscopy (AFM) are related to the Na^+ -binding to phospholipids [14–18].

In atomistic resolution molecular dynamics simulations, almost all generally used models seems to predict binding

^{*} The authors are listed in alphabetical order.; The author list is not completed.; University of East Anglia, Norwich, United Kingdom

[†] Helsinki Biophysics and Biomembrane Group, Department of Biomedical Engineering and Computational Science, Aalto University, Espoo, Finland

[‡] Tampere University of Technology, Tampere, Finland

[§] Fachbereich Physik, Freie Universität Berlin, Berlin, Germany

[¶] Institut de Biologie et Chimie des Protéines (IBCP), CNRS UMR 5086, Lyon, France

^{**} Aalto University, Espoo, Finland

^{††} University of East Anglia, Norwich, United Kingdom

^{‡‡} **Author to whom correspondence may be addressed. E-mail: samuli.ollila@aalto.fi.**; Department of Neuroscience and Biomedical Engineering, Aalto University, Espoo, Finland



FIG. 1: Chemical structure of 1-palmitoyl-2-oleoylphosphatidylcholine (POPC).

of Na^+ ions into a phosphatidylcholine lipid bilayer, but the strength of binding depends on the model used [12, 13, 22, 24–27]. The reduced lipid lateral diffusion due to Na^+ binding in simulations agrees with fluorescent probe measurements [7, 9, 12], but not with the NMR experiments [11]. The area per lipid reduction due to Na^+ binding in simulations agrees with AFM experiments [14–18], however, the area reduction is observed at significantly too low concentrations when compared with the scattering experiments [10]. The simulations also predict too positive electrophoretic mobility with NaCl compared with experiments, however, this has been explained by the Cl^- ion behaviour [22, 23].

In this work, we resolve these contradictions by directly comparing the headgroup hydrocarbon segment, α and β in Fig. 1, order parameters between simulations and experiments as a function of NaCl and CaCl_2 concentrations. According to the “electrometer concept” the changes of these order parameters can be used to measure the ion affinity to the phosphatidylcholine lipid bilayer [19, 28–30]. Since the order parameters can be accurately measured from experiments and straightforwardly compared to simulations [31], the electrometer concept allows the direct comparison of binding affinity between simulations and experiments. In this work, we show that the qualitative response of order parameters to penetrating cations is correct in simulations, but the Na^+ affinity is significantly overestimated in several molecular dynamics simulation models. Further, the accuracy of tested models do not allow atomistic resolution interpretation of lipid- Ca^{2+} interactions.

II. RESULTS AND DISCUSSION

The electrometer concept is originally based on the measured absolute value increase for β and decrease for α segment order parameters with bound cations [19, 28–30]. However, the later experiments assigned negative sign for β order parameter and positive for α [32–34], thus the both or-

der parameter values are actually decreasing (becoming more negative) with bound cations [31]. The headgroup order parameters values from H^2 NMR [19, 28] together with correct signs [32–34] as a function NaCl and CaCl_2 concentrations for DPPC and POPC bilayers are shown in Fig. 2. Only minute decrease is measured with NaCl while order of magnitude larger effect is observed with CaCl_2 . Thus, according to the electrometer concept monovalent Na^+ ion has negligible lipid bilayer affinity with these concentrations in contrast to multivalent Ca^{2+} ions [19, 28]. This conclusion is in agreement with several other experimental studies [2–4, 10, 11].

The headgroup order parameters in Fig. 2 with added NaCl shows different behaviour for different simulation models. The simulated systems are described in Table I and in Supplementary Information. While all simulation models show order parameter decrease due to Na^+ ion binding, significantly different binding affinities are predicted by different models. This is demonstrated by plotting the density profiles from different models in increasing order according to the observed order parameters changes with NaCl concentration in Fig. 3. The Na^+ density peaks at the lipid bilayer interface clearly increase towards the bottom of the figure, thus correlating with the increased order parameter change. In conclusion, the choline structural response to the Na^+ binding is qualitatively correct and the electrometer concept [19, 28–30] can be used to analyze the Na^+ binding affinity in simulations, despite of the varying quality of the sampled choline and glycerol backbone structures in different simulation models [35].

The lowest Na^+ binding affinities and order parameter changes in best agreement with experiments are seen for the Orange, CHARMM36 and Lipid14 models in Figs. 2 and 3. However, the ion density profiles in Fig. 3 show detectable differences in Na^+ affinity between these models, Orange having lowest affinity and CHARMM36 highest. With the achieved accuracy for the order parameters we are not able to conclude which of these three models has the most realistic Na^+ binding affinity, especially with physiological NaCl concentrations ($\sim 150\text{mM}$) which is most relevant for most applications. On the other hand, the choline order parameter changes with NaCl are clearly overestimated in all the other studied models indicating unrealistically strong Na^+ binding affinity to the bilayer. This is manifested by the density peaks in Fig. 3, seen also with physiological concentrations.

The overestimated Na^+ binding may originate, e.g., from incorrect choline structure [35], lack of polarizability [87], other discrepancies in the ion models [88–90] or from combination of these and other issues. Interestingly, the same ion model and non-bonded parameters are used in the Orange and BergerOPLS [45] simulations while Na^+ ion binding affinity is realistic in the Orange model but overestimated in BergerOPLS model. This shows that the binding affinity significantly depends on the used lipid parameters. On the other hand, Na^+ binding with Berger, BergerOPLS and Slipid models is reduced but not yet agree with experiments by using the ion models with scaled charges to compensate the electronic polarizability [87, 91], see Supplementary Information. Further, Slipid model gives similar binding affinity with two different ion parameters. These results indicate that at least lipid mod-

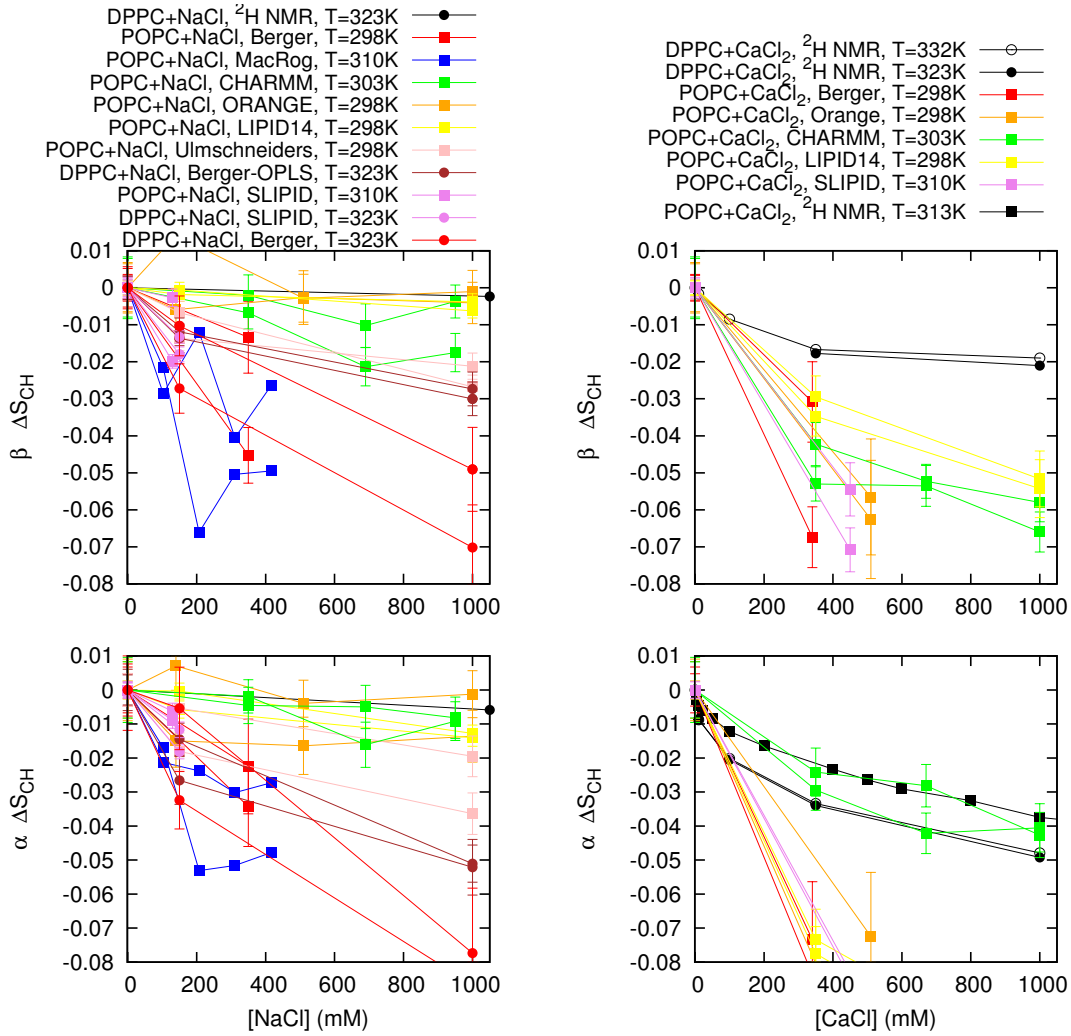


FIG. 2: The order parameter changes for β and α segments as a function of NaCl (left column) and CaCl₂ (right column) concentrations from simulations and experiments [19] (POPC with CaCl₂ from [28]). The signs of the experimental order parameters, taken from experiments without ions [32–34], can be assumed to be unchanged with concentrations represented here [28, 31]. It should be noted that none of the models used here reproduces the order parameters within experimental error for pure PC bilayer without ions, indicating structural inaccuracies with varying severity for all models [35].

els need improvement to correctly predict the Na⁺ binding affinity.

In contrast to Na⁺, Ca²⁺ binding and related order parameter decrease is seen in experiments [2, 3, 19, 28] and in all tested simulation models, see Figs. 2 and 4. While the significant Ca²⁺ binding affinity to a phosphatidylcholine bilayer at mM concentrations is agreed in the literature, the estimations for lipid/Ca²⁺ stoichiometry vary between 17 and 0.24 [13, 21, 28]. The smallest number (0.24) indicating that one Ca²⁺ ion binds roughly four lipid molecules originates from simulation with Berger model [13]. **1. There is something wrong in these stoichiometry numbers.** The direct comparison of order parameters between different simulation models and experiments in Fig. 2 shows that Ca²⁺ binding induced changes are overestimated in all tested models. In contrast to Na⁺, clear correlation between Ca²⁺ binding affinity and order parameter changes is not found, thus the overestimation of order

parameter change may arise, e.g. from overestimated binding, incorrect headgroup response to penetrating divalent cation or penetration depth. The ion model having scaled charges [75] used with CHARMM36 did not improve the results, see Supplementary Information.

The Berger model predicts deeper penetration depth (density maxima close to ± 1.8 nm) compared to other models (density maxima close to ± 2 nm). The latter value is probably more realistic since ¹H NMR and neutron scattering data indicates that Ca²⁺ interact mainly with the choline group [2, 92–94]. Further, the ¹H NMR experiments suggest that the N- β - α -O dihedral is only in gauche-conformation in the absence of ions, but in the presence of multivalent ions also anti-conformations would be present [93, 95]. However, the glycerol backbone and headgroup atomistic resolution structures [35] and their changes are not reproduced within experimental error in the tested simulation models, thus the model

TABLE I: Simulated lipid bilayers with ions. The ion concentrations are the concentration of ions in buffer to solute the lipid bilayers and calculated as $[\text{ion}] = (N_{\text{ion}} \times [\text{water}]) / N_w$, where $[\text{water}] = 55.5\text{M}$. These correspond the concentrations reported in the experiments by Akutsu et al. [19]. The lipid force field parameters are denominated as in previous work [35]. For ion force field parameters the general force field for non-bonded parameters is mentioned and the citation to specific ion parameters is then given, if available.

Force field (lipid, ion)	lipid	[Ion] mM	^a N _l	^b N _w	^c N _{Na}	^d N _{Ca}	^e N _{Cl}	^f T (K)	^g t _{sim} (ns)	^h t _{anal} (ns)	Files
Berger-POPC-07[36]	POPC	0	128	7290	0	0	0	298	270	240	[37]
Berger-POPC-07[36], ffgmx[38]	POPC	340 (NaCl)	128	7202	44	0	44	298	110	50	[39]
Berger-POPC-07[36], ffgmx[38]	POPC	340 (CaCl ₂)	128	7157	0	44	88	298	108	58	[40]
Berger-DPPC-98[41]	DPPC	0	72	2880	0	0	0	323	60	50	[42]
Berger-DPPC-98[41], ffgmx[38]	DPPC	150 (NaCl)	72	2880	8	0	8	323	120	60	[43]
Berger-DPPC-98[41], ffgmx[38]	DPPC	1000 (NaCl)	72	2778	51	0	51	323	120	60	[44]
BergerOPLS-DPPC-06[45]	DPPC	0	72	2880	0	0	0	323	120	60	[46]
BergerOPLS-DPPC-06[45], OPLS[47]	DPPC	150 (NaCl)	72	2880	8	0	8	323	120	60	[48]
BergerOPLS-DPPC-06[45], OPLS[47]	DPPC	1000 (NaCl)	72	2778	51	0	51	323	120	60	[49]
CHARMM36[50]	POPC	0	72	2242	0	0	0	303	30	20	[51]
CHARMM36[50], CHARMM36[52]	POPC	350 (NaCl)	72	2085	13	0	13	303	80	60	[53]
CHARMM36[50], CHARMM36[52]	POPC	690 (NaCl)	72	2085	26	0	26	303	73	60	[54]
CHARMM36[50], CHARMM36[52]	POPC	950 (NaCl)	72	2168	37	0	37	303	80	60	[55]
CHARMM36[50], CHARMM36	POPC	350 (CaCl ₂)	128	6400	0	35	70	303	200	100	[56]
CHARMM36[50], CHARMM36	POPC	670 (CaCl ₂)	128	6400	0	67	134	303	200	120	[57]
CHARMM36[50], CHARMM36	POPC	1000 (CaCl ₂)	128	6400	0	100	200	303	200	100	[58]
MacRog[59]	POPC	0	288	14400	0	0	0	310	90	40	[60]
MacRog[59], OPLS[47]	POPC	100 (NaCl)	288	14554	27	0	27	310	90	50	[61]
MacRog[59], OPLS[47]	POPC	210 (NaCl)	288	14500	54	0	54	310	90	50	[61]
MacRog[59], OPLS[47]	POPC	310 (NaCl)	288	14446	81	0	81	310	90	50	[61]
MacRog[59], OPLS[47]	POPC	420 (NaCl)	288	14392	108	0	108	310	90	50	[61]
Orange, OPLS[47]	POPC	0	72	2880	0	0	0	298	60	50	[62]
Orange, OPLS[47]	POPC	140 (NaCl)	72	2866	7	0	7	298	120	100	[63]
Orange, OPLS[47]	POPC	510 (NaCl)	72	2802	26	0	26	298	120	100	[64]
Orange, OPLS[47]	POPC	1000 (NaCl)	72	2780	50	0	50	298	120	80	[65]
Orange, OPLS	POPC	510 (CaCl ₂)	72	2802	0	26	52	298	120	60	[66]
Slipid[67]	DPPC	0	128	3840	0	0	0	323	150	100	[68]
Slipid[67], AMBER[69, 70]	DPPC	150 (NaCl)	600	18000	49	0	49	323	100	40	-
Slipid[71]	POPC	0	128	5120	0	0	0	303	200	150	[72]
Slipid[71], AMBER[73]	POPC	130 (NaCl)	200	9000	21	0	21	310	105	100	[74]
Slipid[71], AMBER[75]	POPC	450 (CaCl)	200	9000	0	73	146	310	600	100	[76]
Lipid14 [77], AMBER[47]	POPC	0	128	5120	0	0	0	298	205	200	[78]
Lipid14 [77], AMBER[47]	POPC	150 (NaCl)	128	5120	12	0	12	298	205	200	[79]
Lipid14 [77], AMBER[47]	POPC	1000 (NaCl)	128	5120	77	0	77	298	205	200	[80]
Lipid14 [77], AMBER[47]	POPC	350 (CaCl ₂)	128	6400	0	35	70	298	200	100	[81]
Lipid14 [77], AMBER[47]	POPC	1000 (CaCl ₂)	128	6400	0	100	200	298	200	100	[82]
Ulmschneiders [83], OPLS[47]	POPC	0	128	5120	0	0	0	298.15	205	200	[84]
Ulmschneiders [83], OPLS[47]	POPC	150 (NaCl)	128	5120	12	0	12	298.15	205	200	[85]
Ulmschneiders [83], OPLS[47]	POPC	1000 (NaCl)	128	5120	77	0	77	298.15	205	200	[86]

^a The number of lipid molecules

^b The number of water molecules

^c The number of Na⁺ molecules

^d The number of Ca²⁺ molecules

^e The number of Cl molecules

^f Simulation temperature

^g The total simulation time

^h Time frames used in the analysis

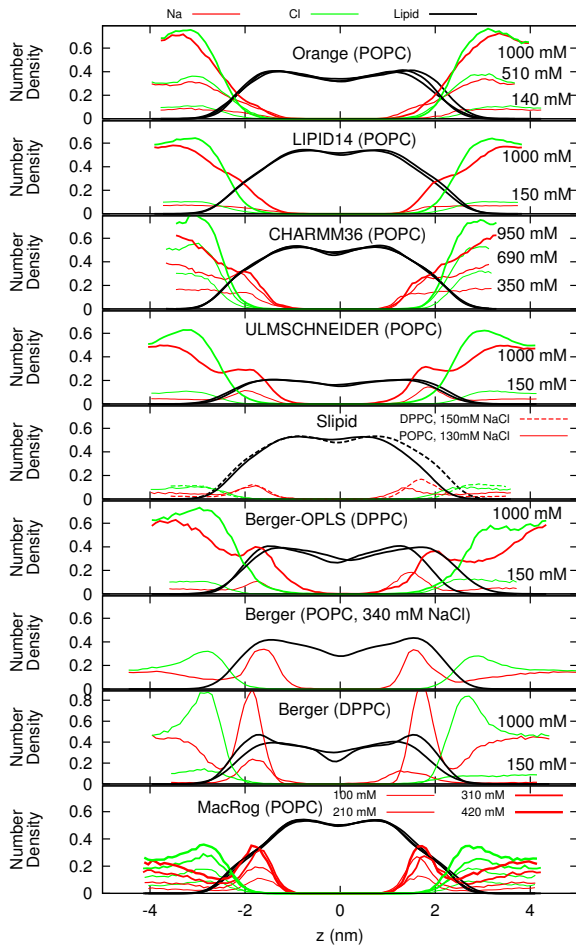


FIG. 3: Atom number density profiles along the membrane normal coordinate z for lipids, Na^+ and Cl^- ions from simulations with different force fields and different NaCl concentrations. The force fields are ordered according to the order parameter changes observed in Fig. 2 such that the models with smallest observed changes are top. The lipid densities are scaled with 100 (united atom) or 200 (all atom model) to make them visible with the used y-axis scale.

Figure discussed in

https://github.com/NMRLipids/lipid_ionINTERACTION/issues/4.

development is needed before Ca^{2+} binding affinity, lipid/ion stoichiometry and concomitant structural changes can be interpreted. **2.The P-N vector tilting analysis should be considered**

III. CONCLUSIONS

As suggested by the electrometer concept [19, 28–30], the headgroup α and β segment order parameter decrease in phosphatidylcholine lipid bilayers is related to the cation binding affinity in all tested simulation models, despite of inaccuracies in actual atomistic resolution structures [35]. The concept allows direct comparison of Na^+ binding affinity between simulations and NMR experiments by using the headgroup or-

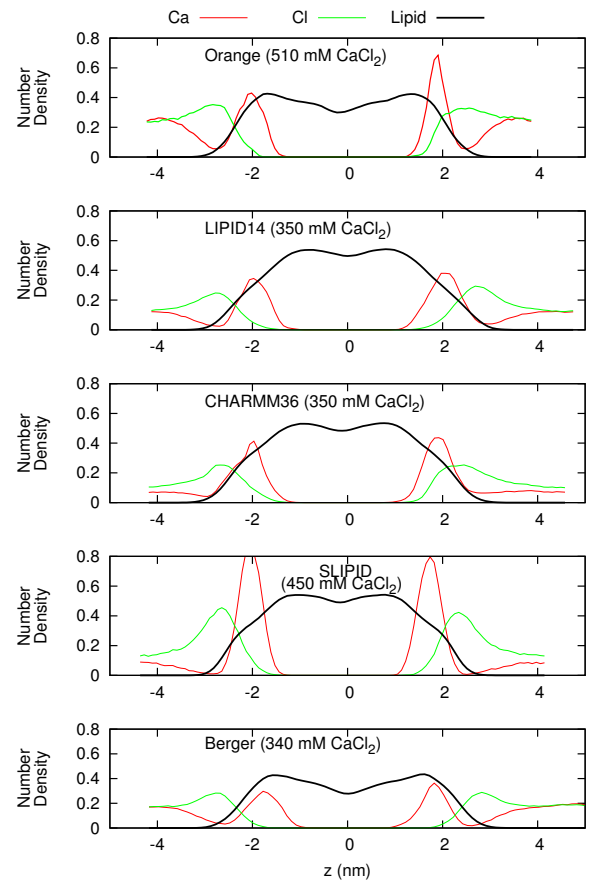


FIG. 4: Atom number density profiles along the membrane normal coordinate z for lipids, Ca^{2+} and Cl^- ions from simulations with different force fields. The profiles only with smallest available CaCl_2 concentration are shown for clarity.

Figure including all the available concentrations is shown in the Supplementary Information. The lipid densities are scaled with 100 (united atom) or 200 (all atom model) to make them visible with the used y-axis scale. Figure discussed in https://github.com/NMRLipids/lipid_ionINTERACTION/issues/4.

der parameter changes. The comparison reveals that most models overestimate the Na^+ binding, only Orange, Lipid14 and CHARMM36 predict realistic binding affinity. None of the tested models has the required accuracy to interpret the Ca^{2+} /lipid stoichiometry or induced atomistic resolution structural changes.

In general the results support the traditional view that Na^+ and other monovalent ions (except Li^+) do not specifically bind to the phospholipid bilayer with mM concentrations, in contrast to Ca^{2+} and other multivalent ions [1, 4, 10, 11, 19–21, 28]. The contradicting results from molecular dynamics simulations [12, 13], fluorescent probe dynamics [7, 9, 12], calorimetry [8, 12] and AFM [14–18] suggesting stronger Na^+ binding can be explained by simulation artefacts, direct interactions between Na^+ and fluorescent probes [11], alternative interpretation of significance of small phase transition temperature shift [2] and insufficient resolution of AFM for

atomistic resolution interpretation.

The artificial specific Na^+ binding in simulations may lead to doubtful results since it leads effectively positively charged phosphatidylcholine lipid bilayer even in physiological NaCl concentration. Such a bilayer has distinctly different interactions with charged objects compared to the more realistic model without specific Na^+ binding. Furthermore, the overestimation of Na^+ binding affinity may extend also to other positively charged objects, e.g. membrane protein segments. This would affect lipid protein interactions and could explain contradicting results on electrostatic interactions between charged protein segments and lipid bilayer [96, 97]. In conclusion, more careful studies and model development on lipid bilayer-charged object interactions are needed to make molecular dynamics simulations straightforwardly usable in physiologically relevant electrostatic environment.

This work has been, and will be, progressed and discussed through the blog: nmrlipids.blogspot.fi. Everyone is invited to join the discussion and make contributions through the blog. The manuscript will be eventually submitted to an appropriate scientific journal. Everyone who has contributed to the work through the blog will be offered coauthorship. For more details see: nmrlipids.blogspot.fi.

Acknowledgements: OHSO acknowledges Tiago Ferreira for very useful discussions, the Emil Aaltonen foundation for financial support, Aalto Science-IT project and CSC-IT Center for Science for computational resources. MSM acknowledges financial support from the Volkswagen Foundation (86110).

SUPPLEMENTARY INFORMATION

Appendix A: Effect of ion model and polarization

It has been suggested that the missing electronic polarizability can be compensated by scaling the ion charge in simulations [87]. To test if this would improve the Na^+ ion binding behaviour, we ran simulations with Berger-DPPC-98, BergerOPLS-DPPC-06 and Slipids with scaled Na^+ and Cl^- ions. For Berger-DPPC-98 and BergerOPLS-DPPC-06 models the ion charge in systems listed in Table I was simply scaled with 0.7 and the related files are available at [98–101]). For simulations with Slipids the ion model by Kohagen et al. was used [91] and the related files are available at [102]. The simulation parameters were identical to those employed in the simulation of POPC with 130 mM NaCl (see Methods). The order parameter changes and Na^+ binding affinity are decreased by the charge scaling but yet overestimated respect to the experiments as seen from Figs. 5 and 6. Thus the overestimated binding affinity cannot be fixed by only scaling charges.

We also tested the effect of charge scaling in the case of CaCl_2 with CHARMM36 model. The ion model by Kohagen et al. [75] was used and the related files are available at [103]. Figures 5 and 7 show that the scaling does not improve the CaCl_2 binding behaviour respect to the experiments. The same scaled model with Slipid in the main text also overestimated the CaCl_2 effect. However, the effect of scaling cannot be analyzed in this case since Slipid simulation was not ran with non-scaled CaCl_2 model.

Appendix B: Density distributions with different CaCl_2 concentrations

The density distributions with all simulated CaCl_2 concentrations are shown in Fig. 7.

Appendix C: methods

1. Simulated systems

All simulations are ran with a standard setup for planar lipid bilayer in zero tension with periodic boundary conditions with Gromacs software package (version numbers 4.5-X-5.0.X).

2. Analysis

The order parameters were calculated from simulation trajectories directly applying the equation $S_{\text{CH}} = \langle \frac{3}{2} \cos^2 \theta - \frac{1}{2} \rangle$, where θ is the angle between a given C–H bond and the bilayer normal and average is taken over all lipids and timeframes. For united atom models the hydrogen locations were regenerated for each molecule in each frame by using the *protonate*

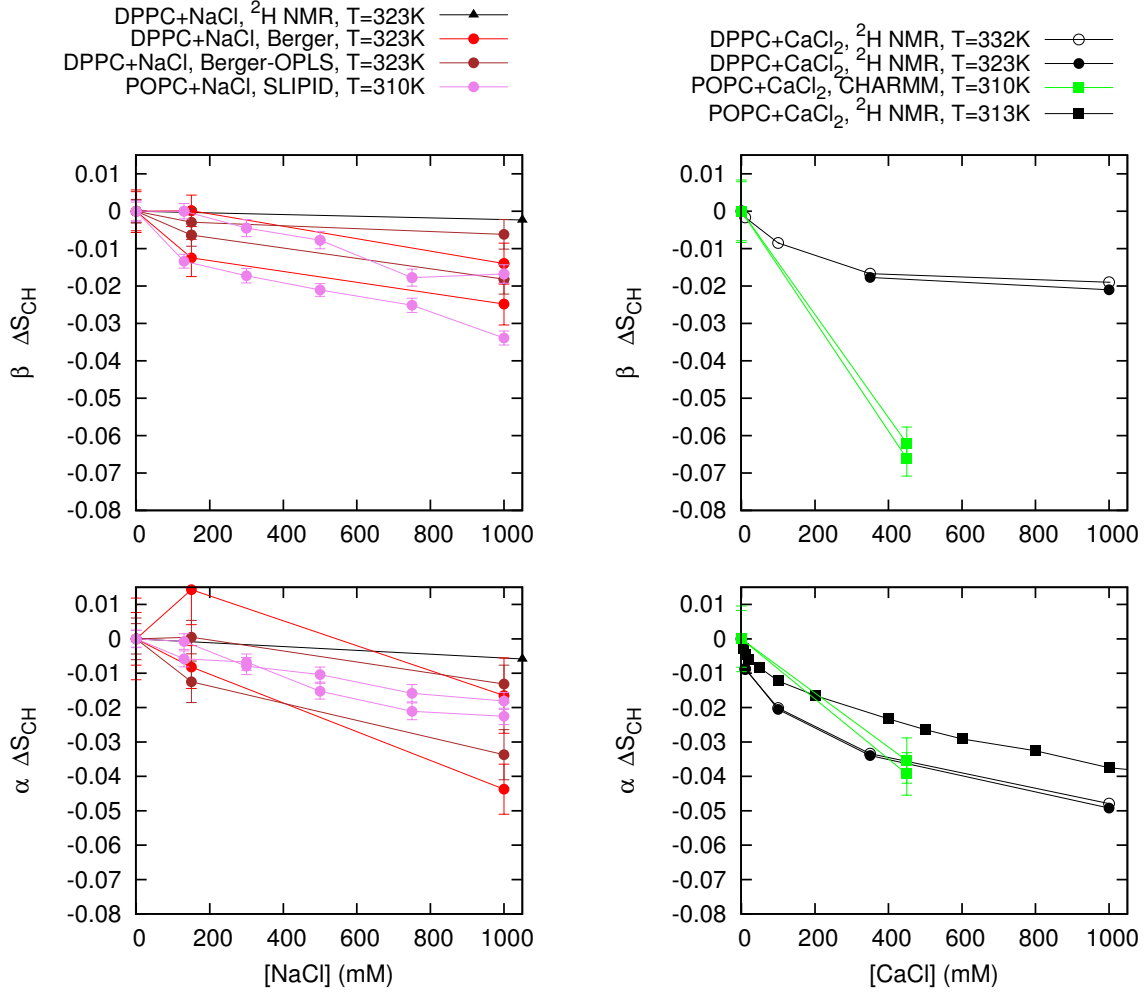


FIG. 5: Order parameter changes in simulations using ion models with scaled charge.

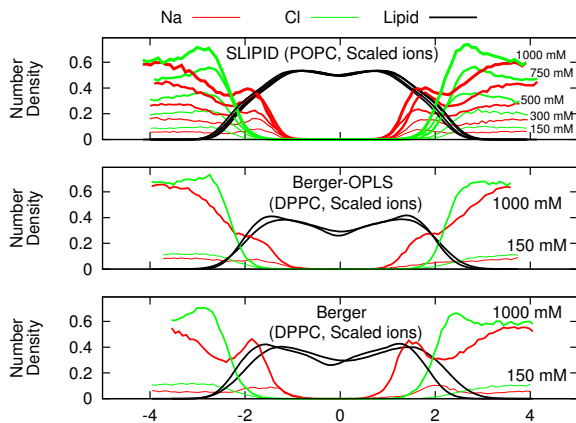


FIG. 6: Atom number density profiles along membrane normal coordinate z for lipids, Na^+ and Cl^- ions from simulations using ion models with scaled charges. The lipid densities are scaled with 100 (united atom) or 200 (all atom model) to make them visible with the used y-axis scale.

tool in Gromacs 4.0.2 [104]. For statistical error estimate order parameter for each lipid molecule was separately calculated and the error of the mean over these values was used as done also in the previous work [35]. All the scripts used in analysis and the resulting data are available in the GitHub repository [105]

3. Simulation details

a. Berger

POPC The simulation without ions is the same as in [106] and the files are available from [37]. The starting structures for simulations with ions is made by replacing water molecules with appropriate amount of ions. The Berger force field was used for the POPC [107], with the dihedral potential next to the double bond taken from [108]. The ion parameters from ffmgx [38] were used. Timestep of 2 fs was used with leapfrog integrator. Covalent bond lengths were constrained with

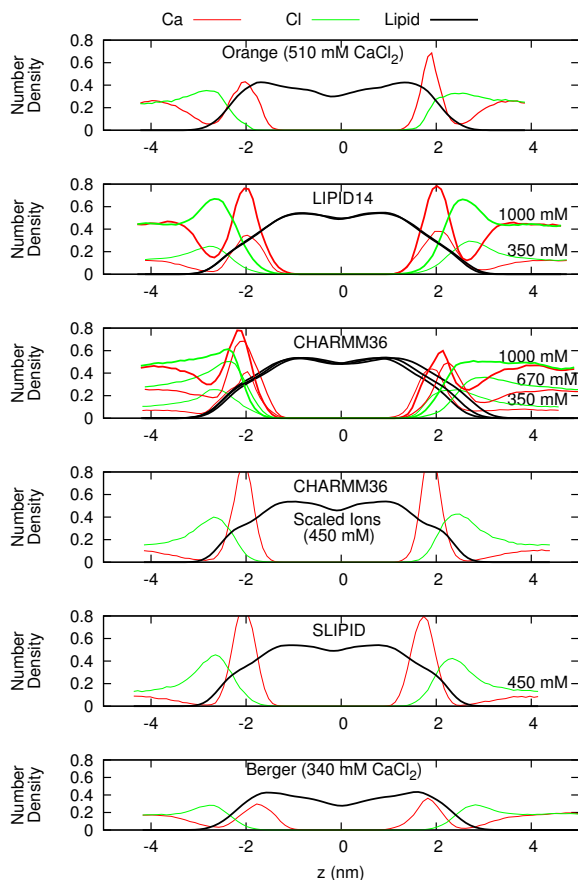


FIG. 7: Number density profiles for lipids, Ca^{2+} and Cl^- ions from simulations with different force fields and different CaCl_2 concentrations. The lipid densities are scaled with 100 (united atom) or 200 (all atom model) to make them visible with the used y-axis scale. Figure discussed in https://github.com/NMRLipids/lipid_ionINTERACTION/issues/4

LINCS algorithm [109, 110]. Coordinates were written every 10 ps. PME [111, 112] with real space cut-off 1.0 nm was used for electrostatics. Plain cut-off was used for the Lennard-Jones interactions with a 1.0 nm cut-off. The neighbour list was updated every 5th step with cut-off 1.0 nm. Temperature was coupled separately for lipids, water and ions to 298 K with the velocity-rescale method [113] with coupling constant 0.1 ps^{-1} . Pressure was semi-isotropically coupled to the atmospheric pressure with the Parrinello-Rahman barostat [114].

DPPC The simulation without ions is the same as in [35] and the files are available from [42]. **3.Simulation details from Jukka Määttä**

b. BergerOPLS

4.Simulation details from Jukka Määttä

c. CHARMM36

POPC with NaCl The simulation without ions is taken directly from [35, 51]. The starting structures for simulations with NaCl were made by replacing randomly located water molecules of the structure of pure POPC simulation with appropriate amount of ions. The force field for lipid were the same as in [35, 51]. The ion parameters with NBFIX by Venable et al. [52] were used. Simulations were ran with Gromacs 4.5.5 software [115]. Timestep of 2 fs was used with leap-frog integrator. Covalent bonds with hydrogens were constrained with LINCS algorithm [109, 110]. Coordinates were written every 5 ps. PME with real space cut-off 1.4 nm was used for electrostatics. Lennard-Jones interactions were switched to zero between 0.8 nm and 1.2 nm. The neighbour list was updated every 5th step with cut-off 1.4 nm. Temperature was coupled separately for lipids and solution to 303 K with the velocity-rescale method [113] with coupling constant 0.2 ps. Pressure was semi-isotropically coupled to the atmospheric pressure with the Berendsen method [116].

POPC with CaCl_2 The starting structures with varying amounts of CaCl_2 ions were constructed using the CHARMM-GUI Membrane Builder (<http://www.charmm-gui.org/>) online tool [117]. All runs were performed with Gromacs 5.0.3 software package [118] and CHARMM36 additive force field parameters for lipids [50] and ions were obtained from CHARMM-GUI input files. Standard CHARMM-GUI mdp options were used. Particularly, h-bond lengths were constrained with LINCS [109, 110]. The temperatures of the lipids and the solvent were separately coupled to the Nose-Hoover [119, 120] thermostat with a target temperature of 303 K and a relaxation time constant of 1.0 ps. Semi-isotropic pressure coupling to 1 bar was obtained with the Parrinello-Rahman barostat [114] with a time constant of 5 ps. Equations of motion were integrated with the Verlet algorithm [121] using a timestep of 2 fs. Long-range electrostatic interactions were calculated using the PME [111, 112] method with a fourth order smoothing spline. A real space cut-off of 1.2 nm was employed with grid spacing of 0.12 nm in the reciprocal space. Lennard-Jones interactions were smoothly switched to zero between 1.0 nm and 1.2 nm. Verlet cutoff-scheme [121] were used with the long-range neighbor list updated every 20 steps. Coordinates were written every 10 ps. After energy minimization and an equilibration run of 0.5 ns, 200ns simulations were ran and the last 100ns of each simulation was employed for the analysis.

d. MacRog

The simulation parameters are identical to those employed in our earlier study [35] for the full hydration and dehydration simulations. The initial structures with varying amounts of NaCl were constructed from an extensively hydrated bilayer by replacing water molecules with ions using the Gromacs tool genion [122]. Even at the highest considered salt concentration, the amount of water molecules per lipid after this replacement process was still greater than 50.

e. Orange

5.Jukka Maatta and Luca Monticelli, please deliver as much details as you can.

f. Slipids

DPPC The simulation without ions from [35], available at [68] was used. For the simulations with ions, the starting DPPC lipid bilayer, which was built with the online CHARMM-GUI [117] (<http://www.charmm-gui.org/>), contained 600 lipids, 30 water molecules/lipid, Na^+ and Cl^- ions (150 mM NaCl). The TIP3P water model was used to solvate the system and ion parameters by Roux [69, 70] were used. the GROMACS software package version 4.5.5 [115] and the Stockholm lipids (Slipids) force field parameters for phospholipids were used. After energy minimization and a short equilibration run of 50 ps (time step 1 fs), 100 ns production runs were performed using a time step of 2 fs with leapfrog integrator. All covalent bonds were constrained with the LINCS [109, 110] algorithm. Coordinates were written every 100 ps. PME [111, 112] with real space cut-off at 1.0 nm was used for Coulomb interactions. Lennard-Jones interactions were switched to zero between 1.0 nm and 1.4 nm. The neighbour lists were updated every 10^{th} step with a cut-off of 1.6 nm. Temperature was coupled separately for upper and bottom leaflets of the lipid bilayer, and for water to one of the temperatures reported above with the Nosé-Hoover thermostat [119, 120] using a time constant of 0.5 ps. Pressure was semi-isotropically coupled to the atmospheric pressure with the Parrinello-Rahman [114] barostat using a time constant of 10 ps.

POPC The simulation without ions from [35], available at [72] was used. Additionally, a POPC bilayer consisting of 200 lipids, hydrated with 45 water molecules per lipid, was simulated in the presence of 130 mM NaCl. **6.Details from the simulation with CaCl** The Slipids model [67, 71] was employed for lipids, the tip3p model [123] for water, and the ion parameters by Smith and Dang [73] for NaCl. The system was first equilibrated for 5 ns with a time step of 1 fs after which a 100 ns production run was performed using a time step of 2 fs. Trajectories were written every 100 ps. The system was kept in a tensionless state at 1 bar using a semi-isotropical Parrinello-Rahman barostat [114] with a time constant of 1 ps. The temperature was maintained at 310 K with the velocity rescaling thermostat [113]. The time constant was set to 0.5 ps for both lipids and solvent (water and ions) which were coupled separately. Non-bonded interactions were calculated within a neighbor list with a radius of 1 nm and an update interval of 10 steps. The Lennard-Jones interactions were cut-off at 1 nm, whereas PME [111, 112] was employed for long-range electrostatics. Dispersion correction was applied to both energy and pressure. All bonds were constrained with the LINCS [109, 110]. algorithm.

g. Lipid14

The starting structures with varying amounts of ions were constructed using the CHARMM-GUI Membrane Builder (<http://www.charmm-gui.org/>) online tool [117]. The GROMACS compatible force field parameters generated in [35] and available at [124] were used. The TIP3P water model [123] was used to solvate the system and Åqvist [47] parameters were used for ions. All runs were performed with Gromacs 5.0.3 software package [118] and LIPID14 force field parameters for POPC [77].

H-bond lengths were constrained with LINCS [109, 110]. The temperatures of the lipids and the solvent were separately coupled to the Nose-Hoover [119, 120] thermostat with a target temperature of 298.15 K and a relaxation time constant of 0.1 ps. Semi-isotropical pressure coupling to 1 bar was obtained with the Parrinello-Rahman barostat [114] with a time constant of 2 ps. Equations of motion were integrated with the Verlet algorithm [121] using a timestep of 2 fs. Long-range electrostatic interactions were calculated using the PME [111, 112] method with a fourth order smoothing spline. A real space cut-off of 1.0 nm was employed with grid spacing of 0.12 nm in the reciprocal space. Lennard-Jones potentials were cut-off at 1 nm, with a dispersion correction applied to both energy and pressure. Verlet cutoff-scheme [121] were used with the long-range neighbor list updated every 20 steps. Coordinates were written every 10 ps.

After energy minimization and an equilibration run of 5 ns, 200ns production runs were performed and analysed. In case of the CaCl_2 systems only the last 100ns of each simulation was employed for the analysis.

h. Ulmsneiders

The starting structures with varying amounts of ions were constructed using the CHARMM-GUI Membrane Builder (<http://www.charmm-gui.org/>) online tool [117]. The force field parameters were obtained from Lipidbook [125]. The TIP3P water model [123] was used to solvate the system. Additionally, the simulations of ion-free bilayer were repeated with both Verlet and Group cutoff-schemes [84]. There was no significant difference in headgroup or glycerol backbone order parameters between these cutoff-schemes. All runs were performed with Gromacs 5.0.3 software package [118]. The glycerol backbone order parameters without iones were not the same as reported in the previous study [35]. The origin of discrepancy was located to the different initial structures which was taken from CHARMM-GUI in this work and from Lipidbook in the previous work. Since the order parameters with the initial structure from CHARMM-GUI are closer to the experimental values, the results indicate that the structure available from Lipidbook is stuck to a state with incorrect glycerol backbone structure, for more discussion see https://github.com/NMRLipids/lipid_ionINTERACTION/issues/8.

All-bond lengths were constrained with LINCS [109, 110]. The temperatures of the lipids and the solvent were sepa-

rately coupled to the Nose-Hoover [119, 120] thermostat with a target temperature of 298.15 K and a relaxation time constant of 0.1 ps. Semi-isotropic pressure coupling to 1 bar was obtained with the Parrinello-Rahman barostat [114] with a time constant of 2 ps. Equations of motion were integrated with the Verlet algorithm [121] using a timestep of 2 fs. Long-range electrostatic interactions were calculated using the PME [111, 112] method with a fourth order smoothing spline. A real space cut-off of 1.0 nm was employed with grid spacing of 0.12 nm in the reciprocal space. Lennard-Jones potentials were cut-off at 1 nm, with a dispersion correction applied to both energy and pressure. Verlet cutoff-scheme [121] were used with the long-range neighbor list updated every 20 steps. Coordinates were written every 10 ps. After energy minimization and an equilibration run of 5 ns, 200ns simulations were ran and the last 100ns of each simulation was employed for the analysis.

Appendix D: Author Contributions

Andrea Catte
Mykhailo Girysh

Matti Javanainen
Markus S. Miettinen
Luca Monticelli
Jukka Määttä
Vasily S. Oganessian
O. H. Samuli Ollila co-designed the project with MSM and managed the work. Ran and analyzed several simulations. Wrote the manuscript.
Joona Tynkkynen

TODO

	P.
1. There is something wrong in these stoichiometry numbers.	3
2. The P-N vector tilting analysis should be considered	5
3. Simulation details from Jukka Määttä	8
4. Simulation details from Jukka Määttä	8
5. Jukka Maatta and Luca Monticelli, please deliver as much details as you can.	9
6. Details from the simulation with CaCl	9

-
- [1] M. Eisenberg, T. Gresalfi, T. Riccio, and S. McLaughlin, *Biochemistry* **18**, 5213 (1979).
 - [2] G. Cevc, *Biochim. Biophys. Acta - Rev. Biomemb.* **1031**, 311 (1990).
 - [3] J.-F. Tocanne and J. Teissi, *Biochimica et Biophysica Acta (BBA) - Reviews on Biomembranes* **1031**, 111 (1990).
 - [4] H. Binder and O. Zschörnig, *Chem. Phys. Lipids* **115**, 39 (2002).
 - [5] J. J. Garcia-Celma, L. Hatahet, W. Kunz, and K. Fendler, *Langmuir* **23**, 10074 (2007).
 - [6] E. Leontidis and A. Aroti, *The Journal of Physical Chemistry B* **113**, 1460 (2009).
 - [7] R. Vacha, S. W. I. Siu, M. Petrov, R. A. Böckmann, J. Barucha-Kraszewska, P. Jurkiewicz, M. Hof, M. L. Berkowitz, and P. Jungwirth, *J. Phys. Chem. A* **113**, 7235 (2009).
 - [8] B. Klasczyk, V. Knecht, R. Lipowsky, and R. Dimova, *Langmuir* **26**, 18951 (2010).
 - [9] F. F. Harb and B. Tinland, *Langmuir* **29**, 5540 (2013).
 - [10] G. Pabst, A. Hodzic, J. Strancar, S. Danner, M. Rappolt, and P. Laggner, *Biophys. J.* **93**, 2688 (2007).
 - [11] A. Filippov, G. Ordd, and G. Lindblom, *Chemistry and Physics of Lipids* **159**, 81 (2009).
 - [12] R. A. Böckmann, A. Hac, T. Heimbürg, and H. Grubmüller, *Biophys. J.* **85**, 1647 (2003).
 - [13] R. A. Böckmann and H. Grubmüller, *Ang. Chem. Int. Ed.* **43**, 1021 (2004).
 - [14] S. Garcia-Manyes, G. Oncins, and F. Sanz, *Biophys. J.* **89**, 1812 (2005).
 - [15] S. Garcia-Manyes, G. Oncins, and F. Sanz, *Electrochimica Acta* **51**, 5029 (2006), ISSN 0013-4686, bioelectrochemistry 2005 Bioelectrochemistry 2005, URL <http://www.sciencedirect.com/science/article/pii/S0013468606002775>.
 - [16] T. Fukuma, M. J. Higgins, and S. P. Jarvis, *Phys. Rev. Lett.* **98**, 106101 (2007).
 - [17] U. Ferber, G. Kaggwa, and S. Jarvis, *European Biophysics Journal* **40**, 329 (2011), ISSN 0175-7571, URL <http://dx.doi.org/10.1007/s00249-010-0650-7>.
 - [18] L. Redondo-Morata, G. Oncins, and F. Sanz, *Biophysical Journal* **102**, 66 (2012).
 - [19] H. Akutsu and J. Seelig, *Biochemistry* **20**, 7366 (1981).
 - [20] R. J. Clarke and C. Lpfert, *Biophysical Journal* **76**, 2614 (1999).
 - [21] S. A. TATULIAN, *European Journal of Biochemistry* **170**, 413 (1987), ISSN 1432-1033, URL <http://dx.doi.org/10.1111/j.1432-1033.1987.tb13715.x>.
 - [22] M. L. Berkowitz, D. L. Bostick, and S. Pandit, *Chem. Rev.* **106**, 1527 (2006).
 - [23] V. Knecht and B. Klasczyk, *Biophys. J.* **104**, 818 (2013).
 - [24] J. N. Sachs, H. Nanda, H. I. Petrache, and T. B. Woolf, *Biophys. J.* **86**, 3772 (2004).
 - [25] A. Cordomi, O. Edholm, and J. J. Perez, *J. Chem. Theo. Comput.* **5**, 2125 (2009).
 - [26] C. Valley, J. Perlmutter, A. Braun, and J. Sachs, *J. Membr. Biol.* **244**, 35 (2011).
 - [27] M. L. Berkowitz and R. Vacha, *Acc. Chem. Res.* **45**, 74 (2012).
 - [28] C. Altenbach and J. Seelig, *Biochemistry* **23**, 3913 (1984).
 - [29] J. Seelig, P. M. MacDonald, and P. G. Scherer, *Biochemistry* **26**, 7535 (1987).
 - [30] P. G. Scherer and J. Seelig, *Biochemistry* **28**, 7720 (1989).
 - [31] O. H. S. Ollila and G. Pabst, *Atomistic resolution structure and dynamics of lipid bilayers in simulations and experiments* (2015), submitted to BBA, URL https://github.com/NMRLipids/NMRLipids_V-Review/blob/master/Manuscript/review_manu.pdf.
 - [32] M. Hong, K. Schmidt-Rohr, and A. Pines, *Journal of the American Chemical Society* **117**, 3310 (1995).

- [33] M. Hong, K. Schmidt-Rohr, and D. Nanz, *Biophysical Journal* **69**, 1939 (1995).
- [34] J. D. Gross, D. E. Warschawski, and R. G. Griffin, *Journal of the American Chemical Society* **119**, 796 (1997).
- [35] A. Botan, A. Catte, F. Favela, P. Fuchs, M. Javanainen, W. Kulig, A. Lamberg, M. S. Miettinen, L. Monticelli, J. Määttä, et al., *Towards atomistic resolution structure of phosphatidylcholine glycerol backbone and choline headgroup at different ambient conditions*, <http://arxiv.org/abs/1309.2131v2> (2015), nMRLipids project, nmrlipids.blogspot.fi, 1309.2131.
- [36] S. Ollila, M. T. Hyvönen, and I. Vattulainen, *J. Phys. Chem. B* **111**, 3139 (2007).
- [37] O. H. S. Ollila, T. Ferreira, and D. Topgaard (2014), URL <http://dx.doi.org/10.5281/zenodo.13279>.
- [38] T. P. Straatsma and H. J. C. Berendsen, *The Journal of Chemical Physics* **89** (1988).
- [39] O. O. H. Samuli, *MD simulation trajectory and related files for POPC bilayer with 340mM NaCl (Berger model delivered by Tieleman, ffgmx ions, Gromacs 4.5)* (2015), URL <http://dx.doi.org/10.5281/zenodo.32144>.
- [40] O. O. H. Samuli, *MD simulation trajectory and related files for POPC bilayer with 340mM CaCl₂ (Berger model delivered by Tieleman, ffgmx ions, Gromacs 4.5)* (2015), URL <http://dx.doi.org/10.5281/zenodo.32173>.
- [41] S.-J. Marrink, O. Berger, P. Tieleman, and F. Jähnig, *Biophysical Journal* **74**, 931 (1998).
- [42] J. Määttä (2015), URL <http://dx.doi.org/10.5281/zenodo.13934>.
- [43] J. Mtt, *Dppc.berger.nacl* (2015), URL <http://dx.doi.org/10.5281/zenodo.16319>.
- [44] J. Määttä, *Dppc.berger.nacl.1mol* (2015), URL <http://dx.doi.org/10.5281/zenodo.17210>.
- [45] D. P. Tieleman, J. L. MacCallum, W. L. Ash, C. Kandt, Z. Xu, and L. Monticelli, *J. Phys. Condens. Matter* **18**, S1221 (2006).
- [46] J. Määttä, *Dppc.berger.opls06* (2015), URL <http://dx.doi.org/10.5281/zenodo.17237>.
- [47] J. Åqvist, *The Journal of Physical Chemistry* **94**, 8021 (1990).
- [48] J. Määttä, *Dppc.berger.opls06.nacl* (2015), URL <http://dx.doi.org/10.5281/zenodo.16484>.
- [49] J. Määttä, *Dppc.berger.opls06.nacl.1mol* (2015), URL <http://dx.doi.org/10.5281/zenodo.17208>.
- [50] J. B. Klauda, R. M. Venable, J. A. Freites, J. W. O'Connor, D. J. Tobias, C. Mondragon-Ramirez, I. Vorobyov, A. D. M. Jr. and R. W. Pastor, *J. Phys. Chem. B* **114**, 7830 (2010).
- [51] O. O. H. Samuli and M. Miettinen (2015), URL <http://dx.doi.org/10.5281/zenodo.13944>.
- [52] R. M. Venable, Y. Luo, K. Gawrisch, B. Roux, and R. W. Pastor, *The Journal of Physical Chemistry B* **117**, 10183 (2013).
- [53] S. Ollila, *MD simulation trajectory and related files for POPC bilayer with 350mM NaCl (CHARMM36, Gromacs 4.5)* (2015), URL <http://dx.doi.org/10.5281/zenodo.32496>.
- [54] S. Ollila, *MD simulation trajectory and related files for POPC bilayer with 690mM NaCl (CHARMM36, Gromacs 4.5)* (2015), URL <http://dx.doi.org/10.5281/zenodo.32497>.
- [55] S. Ollila, *MD simulation trajectory and related files for POPC bilayer with 950mM NaCl (CHARMM36, Gromacs 4.5)* (2015), URL <http://dx.doi.org/10.5281/zenodo.32498>.
- [56] G. Mykhailo and O. O. H. Samuli, *Popc.charmm36.cacl2.035mol* (2015), URL <http://dx.doi.org/10.5281/zenodo.35159>.
- [57] G. Mykhailo and O. O. H. Samuli, *Popc.charmm36.cacl2.067mol* (2015), URL <http://dx.doi.org/10.5281/zenodo.35160>.
- [58] G. Mykhailo and O. O. H. Samuli, *Popc.charmm36.cacl2.1mol* (2015), URL <http://dx.doi.org/10.5281/zenodo.35156>.
- [59] A. Maciejewski, M. Pasenkiewicz-Gierula, O. Cramariuc, I. Vattulainen, and T. Rog, *The Journal of Physical Chemistry B* **118**, 4571 (2014).
- [60] M. Javanainen (2014), URL <http://dx.doi.org/10.5281/zenodo.13498>.
- [61] M. Javanainen, *POPC @ 310K, varying amounts of NaCl. Model by Maciejewski and Rog* (2015), URL <http://dx.doi.org/10.5281/zenodo.14976>.
- [62] O. H. S. Ollila, J. Mtt, and L. Monticelli, *MD simulation trajectory for POPC bilayer (Orange, Gromacs 4.5.)* (2015), URL <http://dx.doi.org/10.5281/zenodo.34488>.
- [63] O. H. S. Ollila, J. Mtt, and L. Monticelli, *MD simulation trajectory for POPC bilayer with 140mM NaCl (Orange, Gromacs 4.5.)* (2015), URL <http://dx.doi.org/10.5281/zenodo.34491>.
- [64] O. H. S. Ollila, J. Mtt, and L. Monticelli, *MD simulation trajectory for POPC bilayer with 510mM NaCl (Orange, Gromacs 4.5.)* (2015), URL <http://dx.doi.org/10.5281/zenodo.34490>.
- [65] S. Ollila, J. Mtt, and L. Monticelli, *MD simulation trajectory for POPC bilayer with 1000mM NaCl (Orange, Gromacs 4.5.)* (2015), URL <http://dx.doi.org/10.5281/zenodo.34497>.
- [66] O. H. S. Ollila, J. Mtt, and L. Monticelli, *MD simulation trajectory for POPC bilayer with 510mM CaCl₂ (Orange, Gromacs 4.5.)* (2015), URL <http://dx.doi.org/10.5281/zenodo.34498>.
- [67] J. P. M. Jämbeck and A. P. Lyubartsev, *The Journal of Physical Chemistry B* **116**, 3164 (2012).
- [68] J. Määttä (2014), URL <http://dx.doi.org/10.5281/zenodo.13287>.
- [69] D. Beglov and B. Roux, *The Journal of Chemical Physics* **100** (1994).
- [70] B. Roux, *Biophysical Journal* **71**, 3177 (1996), ISSN 0006-3495, URL <http://www.sciencedirect.com/science/article/pii/S0006349596795115>.
- [71] J. P. M. Jämbeck and A. P. Lyubartsev, *Journal of Chemical Theory and Computation* **8**, 2938 (2012).
- [72] M. Javanainen, *Popc @ 310k, slipids force field*. (2015), DOI: 10.5281/zenodo.13887.
- [73] D. E. Smith and L. X. Dang, *The Journal of Chemical Physics* **100** (1994).
- [74] M. Javanainen, *POPC @ 310K, 130 mM of NaCl. Slipids with ions by Smith & Dang* (2015), URL <http://dx.doi.org/10.5281/zenodo.35275>.
- [75] M. Kohagen, P. E. Mason, and P. Jungwirth, *The Journal of Physical Chemistry B* **118**, 7902 (2014).
- [76] M. Javanainen, *POPC @ 310K, 450 mM of CaCl₂. Slipids with ECC-scaled ions* (2016), URL <http://dx.doi.org/10.5281/zenodo.45007>.
- [77] C. J. Dickson, B. D. Madej, A. Skjevik, R. M. Betz, K. Teigen, I. R. Gould, and R. C. Walker, *Journal of Chemical Theory and Computation* **10**, 865 (2014).
- [78] M. Giryh and O. H. S. Ollila, *Popc.amber.lipid14.verlet* (2015), URL <http://dx.doi.org/10.5281/zenodo.30898>.

- [79] M. Girych and O. H. S. Ollila, *Popc_amber_lipid14_nacl_015mol* (2015), URL <http://dx.doi.org/10.5281/zenodo.30891>.
- [80] M. Girych and O. H. S. Ollila, *Popc_amber_lipid14_nacl_1mol* (2015), URL <http://dx.doi.org/10.5281/zenodo.30865>.
- [81] G. Mykhailo and O. O. H. Samuli, *Popc_amber_lipid14_cacl2_035mol* (2015), URL <http://dx.doi.org/10.5281/zenodo.34415>.
- [82] G. Mykhailo and O. O. H. Samuli, *Popc_amber_lipid14_cacl2_1mol* (2015), URL <http://dx.doi.org/10.5281/zenodo.35074>.
- [83] J. P. Ulmschneider and M. B. Ulmschneider, *Journal of Chemical Theory and Computation* **5**, 1803 (2009).
- [84] M. Girych and O. H. S. Ollila, *Popc_ulmschneider_opls-verlet_group* (2015), URL <http://dx.doi.org/10.5281/zenodo.30904>.
- [85] M. Girych and O. H. S. Ollila, *Popc_ulmschneider_opls_nacl_015mol* (2015), URL <http://dx.doi.org/10.5281/zenodo.30892>.
- [86] M. Girych and O. H. S. Ollila, *Popc_ulmschneider_opls_nacl_1mol* (2015), URL <http://dx.doi.org/10.5281/zenodo.30894>.
- [87] I. Leontyev and A. Stuchebrukhov, *Phys. Chem. Chem. Phys.* **13**, 2613 (2011).
- [88] B. Hess, C. Holm, and N. van der Vegt, *The Journal of Chemical Physics* **124** (2006).
- [89] A. A. Chen, , and R. V. Pappu, *The Journal of Physical Chemistry B* **111**, 11884 (2007).
- [90] M. M. Reif, M. Winger, and C. Oostenbrink, *Journal of Chemical Theory and Computation* **9**, 1247 (2013), pMID: 23418406, <http://dx.doi.org/10.1021/ct300874c>, URL <http://dx.doi.org/10.1021/ct300874c>.
- [91] M. Kohagen, P. E. Mason, and P. Jungwirth, *The Journal of Physical Chemistry B* **0**, null (0), pMID: 26172524, <http://dx.doi.org/10.1021/acs.jpcb.5b05221>, URL <http://dx.doi.org/10.1021/acs.jpcb.5b05221>.
- [92] H. Hauser, M. C. Phillips, B. Levine, and R. Williams, *Nature* **261**, 390 (1976).
- [93] H. Hauser, W. Guyer, B. Levine, P. Skrabal, and R. Williams, *Biochimica et Biophysica Acta (BBA) - Biomembranes* **508**, 450 (1978), ISSN 0005-2736, URL <http://www.sciencedirect.com/science/article/pii/0005273678900913>.
- [94] L. Herbet, C. Napolitano, and R. McDaniel, *Biophysical Journal* **46**, 677 (1984).
- [95] H. Hauser, W. Guyer, and F. Paltauf, *Chemistry and Physics of Lipids* **29**, 103 (1981).
- [96] A. Arkhipov, Y. Shan, R. Das, N. Endres, M. Eastwood, D. Wemmer, J. Kuriyan, and D. Shaw, *Cell* **152**, 557 (2013).
- [97] K. Kaszuba, M. Grzybek, A. Orowski, R. Danne, T. Rg, K. Simons, . Coskun, and I. Vattulainen, *Proceedings of the National Academy of Sciences* **112**, 4334 (2015).
- [98] J. Määttä (2015), URL <http://dx.doi.org/10.5281/zenodo.16320>.
- [99] J. Määttä, *Dppc_berger_nacl_1mol_scaled* (2015), URL <http://dx.doi.org/10.5281/zenodo.17228>.
- [100] J. Määttä (2015), URL <http://dx.doi.org/10.5281/zenodo.16485>.
- [101] J. Mtt, *Dppc_berger_opls06_nacl_1mol_scaled* (2015), URL <http://dx.doi.org/10.5281/zenodo.17209>.
- [102] M. Javanainen, *POPC @ 310K, varying amounts of NaCl. Slipids with ECC-scaled ions* (2015), URL <http://dx.doi.org/10.5281/zenodo.35193>.
- [103] M. Javanainen, *POPC @ 310K, 450 mM of CaCl2. Charmm36 with ECC-scaled ions* (2016), URL <http://dx.doi.org/10.5281/zenodo.45008>.
- [104] D. van der Spoel, E. Lindahl, B. Hess, A. R. van Buuren, E. Apol, P. J. Meulenhoff, D. P. Tieleman, A. L. T. M. Sijbers, K. A. Feenstra, R. van Drunen, et al., *GROMACS user manual version 4.0* (2005), URL www.gromacs.org.
- [105] O. H. S. Ollila and et al. (2015), URL https://github.com/NMRLipids/lipid_ionINTERACTION.
- [106] T. M. Ferreira, F. Coreta-Gomes, O. H. S. Ollila, M. J. Moreno, W. L. C. Vaz, and D. Topgaard, *Phys. Chem. Chem. Phys.* **15**, 1976 (2013).
- [107] O. Berger, O. Edholm, and F. Jähnig, *Biophys. J.* **72**, 2002 (1997).
- [108] M. Bachar, P. Brunelle, D. P. Tieleman, and A. Rauk, *J. Phys. Chem. B* **108**, 7170 (2004).
- [109] B. Hess, H. Bekker, H. J. C. Berendsen, and J. G. E. M. Fraaije, *J. Comput. Chem.* **18**, 1463 (1997).
- [110] B. Hess, *Journal of Chemical Theory and Computation* **4**, 116 (2008).
- [111] T. Darden, D. York, and L. Pedersen, *The Journal of Chemical Physics* **98** (1993).
- [112] U. L. Essman, M. L. Perera, M. L. Berkowitz, T. Larden, H. Lee, and L. G. Pedersen, *J. Chem. Phys.* **103**, 8577 (1995).
- [113] G. Bussi, D. Donadio, and M. Parrinello, *The Journal of Chemical Physics* **126** (2007).
- [114] M. Parrinello and A. Rahman, *J. Appl. Phys.* **52**, 7182 (1981).
- [115] S. Pronk, S. Pli, R. Schulz, P. Larsson, P. Bjelkmar, R. Apostolov, M. R. Shirts, J. C. Smith, P. M. Kasson, D. van der Spoel, et al., *Bioinformatics* **29**, 845 (2013).
- [116] H. J. C. Berendsen, J. P. M. Postma, W. F. van Gunsteren, A. DiNola, and J. R. Haak, *J. Chem. Phys.* **81**, 3684 (1984).
- [117] J. Lee, X. Cheng, J. M. Swails, M. S. Yeom, P. K. Eastman, J. A. Lemkul, S. Wei, J. Buckner, J. C. Jeong, Y. Qi, et al., *Journal of Chemical Theory and Computation* **0**, null (0).
- [118] M. J. Abraham, T. Murtola, R. Schulz, S. Pli, J. C. Smith, B. Hess, and E. Lindahl, *SoftwareX* **12**, 19 (2015), ISSN 2352-7110, URL <http://www.sciencedirect.com/science/article/pii/S2352711015000059>.
- [119] S. Nose, *Mol. Phys.* **52**, 255 (1984).
- [120] W. G. Hoover, *Phys. Rev. A* **31**, 1695 (1985).
- [121] S. Pli and B. Hess, *Computer Physics Communications* **184**, 2641 (2013), ISSN 0010-4655, URL <http://www.sciencedirect.com/science/article/pii/S0010465513001975>.
- [122] M. Abraham, D. van der Spoel, E. Lindahl, B. Hess, and the GROMACS development team, *GROMACS user manual version 5.0.7* (2015), URL www.gromacs.org.
- [123] W. L. Jorgensen, J. Chandrasekhar, J. D. Madura, R. W. Impey, and M. L. Klein, *The Journal of Chemical Physics* **79** (1983).
- [124] O. H. S. Ollila and M. Retegan, *Md simulation trajectory and related files for popc bilayer (lipid14, gromacs 4.5)* (2014), URL <http://dx.doi.org/10.5281/zenodo.12767>.
- [125] J. Domaski, P. Stansfeld, M. Sansom, and O. Beckstein, *The Journal of Membrane Biology* **236**, 255 (2010), ISSN 0022-2631.